

Diagnostic information contained in inter-harmonics of a direct and PWM supplied induction machine

Jan Rusek

Chair of Electrical Machines

AGH University of Science and Technology

Al. Mickiewicza 30, 30-059 Krakow (Poland)

phone: +48 126172897, fax: +48 126341096, e-mail: gerusek@cyf-kr.edu.pl

Abstract.

The paper contains waveforms of currents for the direct and voltage source inverter supplied induction machine, with account for harmonics and inter-harmonics. By direct supply the grid is assumed to be polluted by 3rd, 5th and 7th harmonics, normally present in real power supply systems. The voltage inverter was assumed to operate in a PWM mode, with perfectly constant DC link current. Spectrums of stator currents for direct supply create reference bases for spectrums by PWM supply.

The model of the machine accounts for dependencies of stator and rotor inductances on rotor angle, resulting from winding and air gap geometry. Calculations of the derivatives of inductances, with respect to rotor angle, allowed for calculation of electromagnetic torque and machine's dynamics, with allowance for speed fluctuation, also in steady state operation.

Key words

direct and PWM supplied induction machine, spectral composition of currents, inter-harmonics

1. Introduction

The aim of the paper is to calculate waveforms of stator phase and rotor bar currents for a direct or voltage source inverter supplied squirrel cage induction machine, with account for both the harmonics and inter-harmonics. By direct supply the grid is assumed to be polluted by 3rd, 5th and 7th harmonics, normally present in a real power supply system. With account to reality, the 1st, 3rd and 7th harmonics are assumed to constitute positive sequences, whereas the 5th the negative one. The voltage inverter is assumed to operate in a PWM mode. Spectrums of stator currents by direct supply are included, to create a reference bases for current spectrums by PWM supply.

Special model of the machine accounts for true dependencies of stator and rotor inductances on rotor angle, resulting from winding and air gap geometry. Calculations of true derivatives of inductances, with respect to rotor angle, allowed for calculation of electromagnetic torque and, in consequence, the machine's dynamics, with allowance for speed fluctuation also in steady state operation [1].

By PWM supply, the carrier frequency was 5 kHz, and the modulating one 50 Hz. All calculations refer to a 122kW, 1000V, 2p= 4, NS/NR = 72/56 slots machine. The loading torque had T0= 55Nm component independent of speed plus a component depending on the square of the speed, reaching T2= 800Nm by full speed

of 1500 rpm. The inertia was 4.52 + 0.52 kg·m². The model parameters were established on the basis of manufacturer's data, including winding scheme.

2. Direct supply, centrally aligned rotor

Fig.1a shows the startup and steady-state current by a directly supplied machine. Its spectral composition is shown in Fig.1b. Maximum values of phase supply voltages were: 814.56V by 50Hz, 0.4V by 150Hz, 2.2V by 250Hz and 0.5V by 350Hz. Voltage phase shifts were 0,-120,+120 degrees (positive sequence) for 50, 150 and 350Hz and 0,+120,-120 degrees (negative sequence) for 250Hz. Inductances were calculated for 840 rotor positions. The integration step was 2*10⁻⁵s and the printout step was 4*10⁻⁵s.

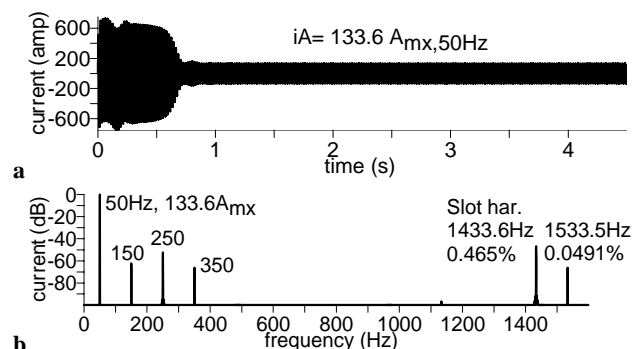


Fig.1. Current and its spectrum, referring to 1.7s - 4.3s segment. $h=1$ [2][3]. Frequency resolution $\Delta f=0.3815\text{Hz}$.

The presence of the 150, 250 and 350Hz harmonics is the consequence of powering by voltages contaminated by higher harmonics. A slot harmonic frequency of 1433.6Hz follows from the harmonic balance model [2]:

$$f_{Slot} = f_1 + h N_R n_{rps} = 50 + 1 \cdot 56 \cdot 24.705 = 1433.48 \text{ Hz} \quad (1)$$

where $f_1 = 50\text{Hz}$, parameter h , following from (31) in [2], is $h=1$, and the speed $n_{rps} = 24.705 \text{ rev./s}$. The discrepancy of 0.12Hz lies within the $\Delta f=0.3815\text{Hz}$ frequency resolution.

Justification for the presence of harmonic 1533.5Hz in Fig.1b is a bit more complex. It follows from (29) in [2], that the frequency of the parasitic synchronous torque is:

$$f_{TqB} = 2f_1 + \beta_B n_{rps} = 2 \cdot 50 + 56 \cdot 24.705 = 1483.48 \text{ Hz} \quad (2)$$

where the parameter β_B results from (27) in [2]:

$$\beta_B = g \cdot N_R = (4 + 6 \cdot k) \cdot p \quad (3)$$

and, with $g = 1$, $k = 4$, amounts to $\beta_B = 56$. This torque harmonic is visible in Fig.2c, and is marked as 1483.5Hz. The discrepancy of 0.1Hz lies within the $\Delta f = 0.3815\text{Hz}$ frequency resolution.

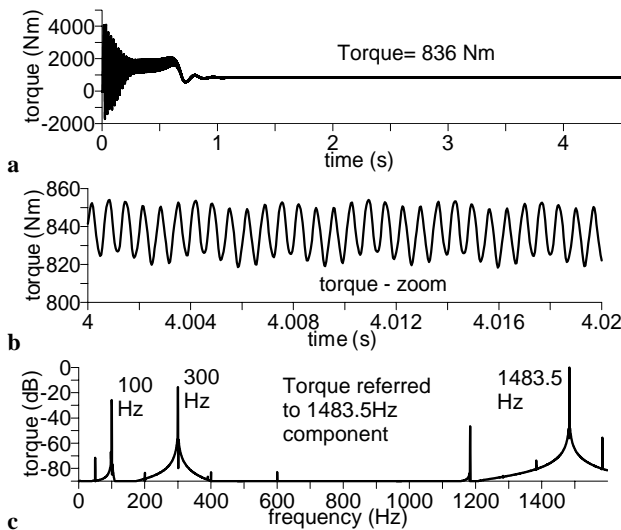


Fig.2. Torque, its zoom and spectrum. $\Delta f = 0.3815\text{Hz}$.

Torque fluctuations are followed by speed fluctuations of the same frequencies, seen in Fig.3.

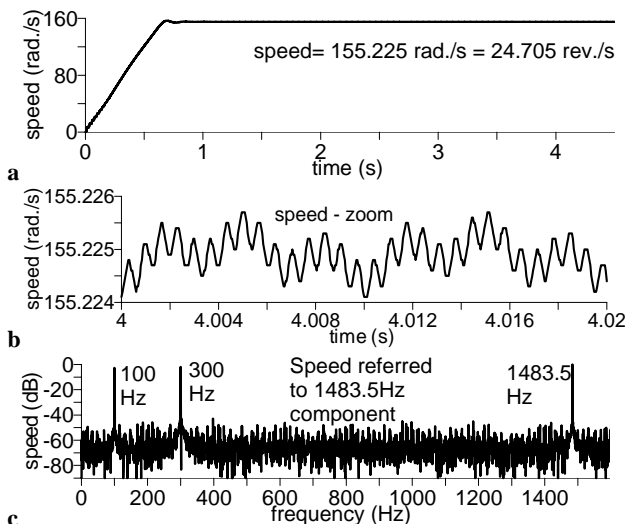


Fig.3. Speed, its zoom and spectrum. $\Delta f = 0.3815\text{Hz}$.

Speed fluctuation of the frequency of 1483.48Hz would cause modulation of the amplitude of the stator current 50Hz component:

$$i(t) = I_1(1 + \cos(2\pi 1483.48)) \cdot \cos(2\pi 50) = I_1 \cos(2\pi 50) + \frac{I_1}{2} \cos(2\pi 1433.48) + \frac{I_1}{2} \cos(2\pi 1533.48) \quad (4)$$

Frequency of the penultimate term in (4) coincides with that of slot harmonic. The last term in (4) gives justification for the harmonic 1533.5Hz in Fig.1b. Hence, the reason for the most right harmonic in Fig.1b is speed fluctuation caused by synchronous parasitic torque. Its presence cannot directly follow from harmonic balance model as it refers to constant speed. Let us remind, the current in Fig.1 results from dynamical model, and not from harmonic balance model. The latter one only unanimously justifies the frequency of the slot harmonic, that is that of 1433.6Hz.

3. Direct supply, 80% static eccentricity

The current, analogous to that in Fig.1a, but now with account for 80% static eccentricity was calculated. Its spectrum is shown in Fig.4. It is evident that static eccentricity is accompanied by a T^{1233.6Hz} Twin harmonic. It is shifted by 100Hz to the left of S or Slot harmonic. The amplitude of the T harmonic is rather small and amounts to -88 dB with respect to L^{50Hz} Line harmonic, despite quite considerable (80%) eccentricity.

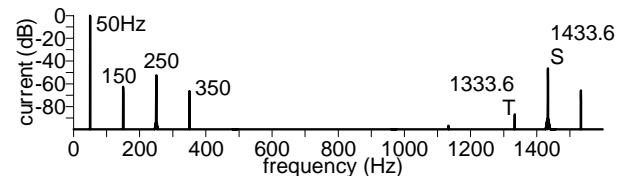


Fig.4. Spectrum of stator current by 80% static eccentricity. $h = 1$. $\Delta f = 0.3815\text{Hz}$.

4. Direct supply, 80% dynamic eccentricity

A current, analogous to that in Fig.1a, but now with account for 80% dynamic eccentricity was calculated. Its spectrum is shown in Fig.5. It is evident that dynamic eccentricity is accompanied by a DT²1282.8Hz harmonic. It is shifted by double rotor speed $2 \cdot n_{\text{tps}}$ (expressed in rev./s) to the right of potential T harmonic. The amplitude of the DT2 harmonic is higher than in the case of static eccentricity and amounts to -80 dB with respect to L^{50Hz} harmonic. Potential T harmonic is not present in spectrums referring to pure dynamic eccentricity, as it accompany static eccentricity. However its frequency is well defined and coincide with that in Fig.4. Hence, the frequency of the DT2 harmonic amounts to:

$$f_{DT2} = 1333.6 + 2 \cdot 24.705 = 1382.01 \text{ Hz} \quad (5)$$

The discrepancy between 1283.01 and 1282.8 lies within the $\Delta f = 0.3815\text{Hz}$ frequency resolution.

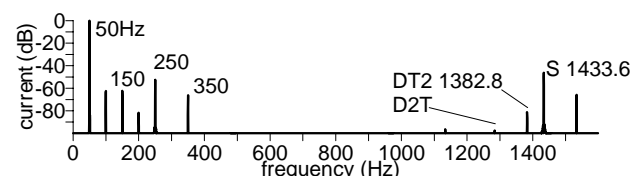


Fig.5. Spectrum of stator current by 80% dynamic eccentricity. $h = 1$. $\Delta f = 0.3815\text{Hz}$.

Dynamic eccentricity is also accompanied by a D2T harmonic, shifted by $2 \cdot n_{\text{tps}}$ to the left of potential T harmonic, though of still smaller amplitude.

5. Direct supply, 40% static + 40% dynamic eccentricity

A current, analogous to that in Fig.1a, but now with account for 40% static + 40% dynamic eccentricity was calculated. Its spectrum is shown in Fig.6. It is evident that the mixed eccentricity is accompanied by a set of characteristic harmonics. Two rotational harmonics, r1L and rL1, appeared in L zone, that is around L^{50Hz} line

harmonic. Their frequencies are 25.177Hz and 74.768Hz. That is they are spaced from L"50Hz by 24.705Hz, that is by rotor speed $n_{tps} = 24.705$ rev./s. Twin harmonic T"1233.6Hz is present due to static eccentricity. It is smaller than in Fig.4, as now the static eccentricity amounts only to 40% and not to 80%. Harmonic DT2 is spaced by $2 \cdot n_{tps}$ to the right of T harmonic, and hence it coincides with harmonic DT2 in Fig.5, characteristic for dynamic eccentricity. Again, the amplitude of harmonic DT2 in Fig.6 is smaller than in Fig.5 as now dynamic eccentricity amounts to only 40% and not to 80%. Around slot harmonic S"1433.6Hz appeared harmonics M1S and MS1 spaced from S harmonic to the left and right by n_{tps} . Harmonic DS2, present in Fig.6 is characteristic for dynamic eccentricity, though it was too small to be visible in Fig.5, referring to pure dynamic eccentricity. This delivers evidence for a general rule that the presence of static eccentricity enhances amplitudes of harmonics characteristic for dynamic eccentricity, and vice versa. Harmonic MT1, characteristic for mixed eccentricity, is shifted by n_{tps} to the right of T harmonic.

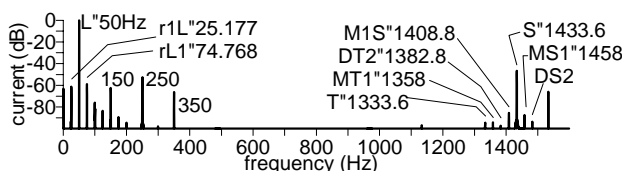


Fig.6. Spectrum of stator current by 40% static + 40% dynamic eccentricity. $h = 1$. $\Delta f = 0.3815$ Hz.

It follows from Fig.6 that the most characteristic harmonics accompanying mixed eccentricity are rotational harmonics r1L and rL1 around fundamental L"50Hz harmonic, as their amplitudes reach -62dB with respect to L"50Hz harmonic. As rotational harmonics r1L and rL1 are absent by pure static (Fig.4) and pure dynamic (Fig.5) eccentricities, it can be concluded that they depend on these eccentricities in a multiplicative and not additive manner [3]. A set of diagnostic harmonics in the 1st slot zone, here, as $h = 1$, coinciding with the main slot zone, though much smaller than the rotational ones in L zone, would enhance the uniqueness and thus the reliability of diagnosis.

4. PWM supply, centrally aligned rotor

The DC intermediate link voltage was assumed to be perfectly constant, and amounted to 1600 volts. The frequency of the carrier saw-tooth wave, common for all three phases, was 5kHz. The frequency of the three sinusoidal modulating waves, spaced by 120 deg., was 50Hz, and their amplitudes, relative to saw-tooth maximum, were 0.9. Fig.7 shows the zoom of half wave of phase-to-phase voltage, calculated on machine's terminals. It coincides with supply voltage delivered by the voltage source inverter in PWM mode. The same supply conditions were assumed for all four cases of rotor eccentricity: none, static, dynamic and mixed. Due to high carrier frequency of 5kHz, it was necessary to lower the integration step down to $h = 2 \cdot 10^{-6}$ s, and print out interval to $8 \cdot 10^{-6}$ s. Fig.8 shows the startup current. Prolonged steady state interval allowed calculation of

stator current spectral composition, shown in Fig.9. The spectrum shows pronounced bunches of harmonics centered around integral multiples of carrier frequency of 5kHz.

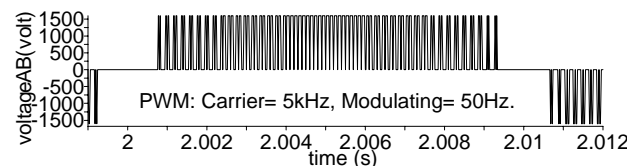


Fig.7. Voltages V_{BC} for the PWM supplied machine with carrier and modulating frequencies $f_c = 5$ kHz and $f_M = 50$ Hz.

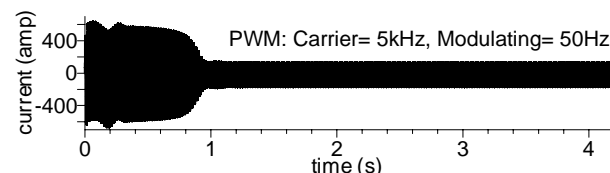


Fig.8. Current by PWM supply ($f_{car} = 5$ kHz). No eccentricity.

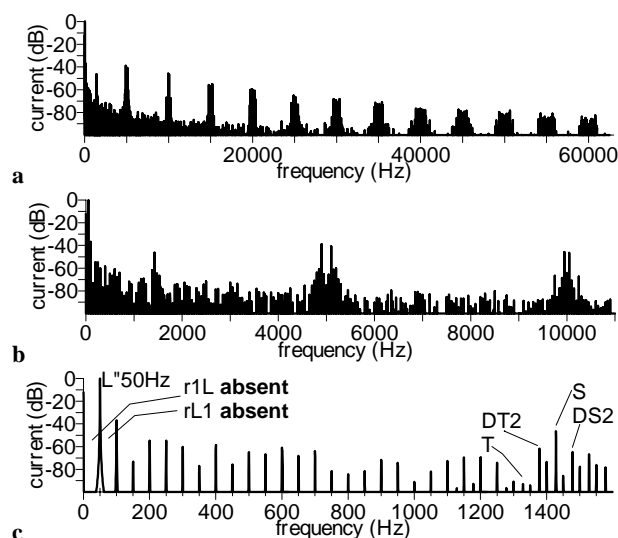


Fig.9. Spectrum of steady-state interval of stator current.

Comparison of Fig.9c with Fig.12c reveals clear difference with respect to rotational harmonics r1L and rL1. These harmonics are not present in Fig.9c as it refers to lack of eccentricity. By direct supply, these harmonics were absent in Fig.1, 4 and 5, and present in Fig.6, proving their origin in mixed eccentricity, as will be the case of Fig.12c.

In Fig.9c, the presence of harmonics T, DT2 and DS2 could be justified as a result of not perfectly symmetrical control of the PWM converter, due to the ratio of carrier and modulating frequencies, as well as assumed control algorithm. Also the integration step of $2 \cdot 10^{-6}$ s might have been still too big. In the case of direct supply these harmonics use to deliver additional evidence for mixed eccentricity, as in Fig.6.

5. PWM supply, 80% static eccentricity

The rotor was assumed to be suspended off stator axis, by 80% of geometrical air gap. The start up current, followed by prolonged steady state current was calculated until 3.8s. Its spectrum, of the steady state interval, is shown in Fig.10. Similarly as in the case of

centric rotor suspension, the rotational harmonics $r1L$ and $rL1$ are absent in Fig.10c. They were present in Fig.6 and will appear in Fig.12c, as they depend multiplicatively on static and dynamic eccentricity.

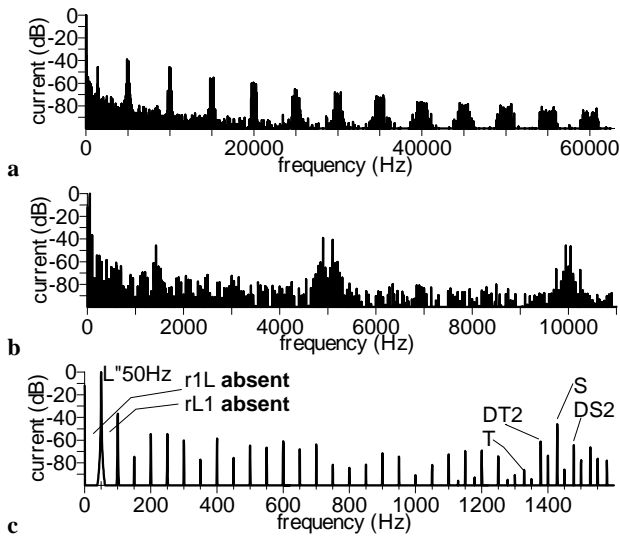


Fig.10. Spectrum of steady-state interval of stator current.

The *twin* harmonic T in Fig10c is considerably greater than that in Fig. 9c. This proves its dependence primarily on static eccentricity. Similarly as in Fig.9c, the presence of harmonics DT2 and DS2 is probably the result of imperfections of the assumed control and integration strategies, in the conditions of PWM supply.

6. PWM supply, 80% dynamic eccentricity

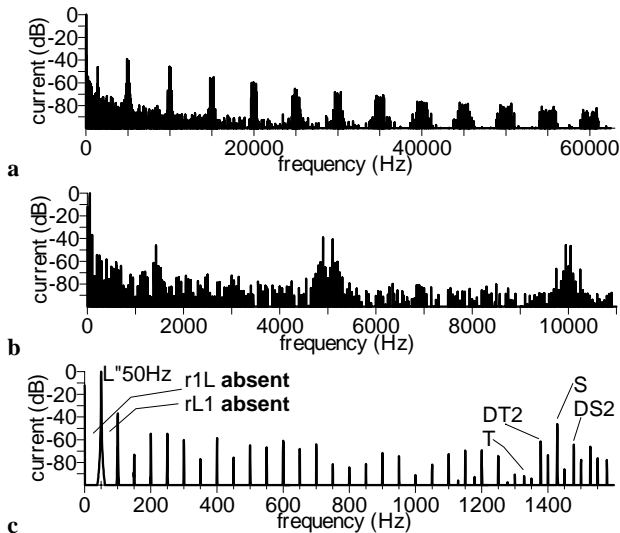


Fig.11. Spectrum of steady-state interval of stator current.

The axis of rotation of the rotor was assumed to be shifted by 80% of geometrical air gap off the rotor axis of geometrical symmetry. The axis of rotor rotation coincides with the stator axis. The start up current, followed by prolonged steady state current was calculated until 3.8s. Its spectrum, of the steady state interval, is shown in Fig.11. The rotational harmonics $r1L$ and $rL1$ are absent, as they depend multiplicatively on static and dynamic eccentricity. It should be stressed that the rotational harmonics are absent despite as high dynamic eccentricity as 80% of air gap.

7. PWM supply, 40% static + 40% dynamic eccentricity

Fig.12 shows the current of the PWM powered machine, for the case of mixed eccentricity. The overall shape of the current is similar to that in Fig.8, although the print out interval was here lowered down to $2 \cdot 10^{-6}$ s, to coincide with integration step $h = 2 \cdot 10^{-6}$ s. The spectrum in Fig.12c shows up harmonics $r1L$ and $rL1$, characteristic for mixed eccentricity, absent in Figs. 9, 10 and 11. Harmonics T, DT2 and DS2 coincide with those in Fig.6.

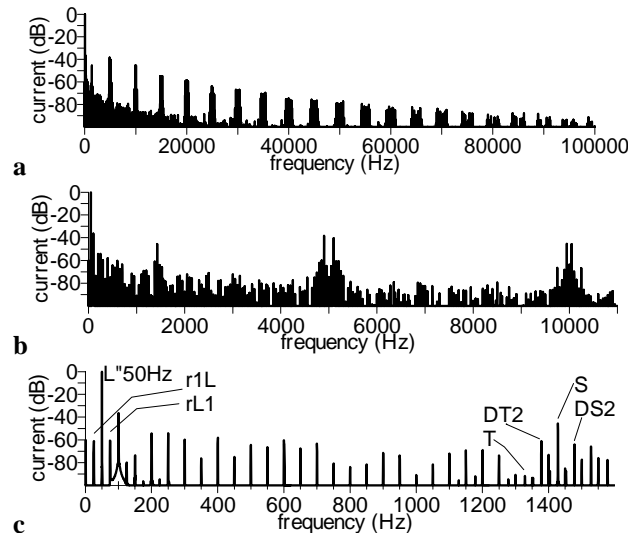


Fig.12. Spectrum of steady-state interval of stator current.

8. Conclusions

1. Rotational harmonics, those around 50Hz, depend multiplicatively on static and dynamic eccentricities. They are only present by mixed eccentricity, that is by simultaneous presence of static and dynamic eccentricity.
2. By direct supply, diagnosing of pure static or pure dynamic eccentricity can be based on characteristic harmonics in slot zone.
3. By PWM supply, distinguishing of the harmonics characteristic to pure static or pure dynamic eccentricity remains still an open issue.
4. Mixed eccentricity rotational harmonics are clearly distinguishable also in case of PWM supply.

References

- [1] Rusek, J.: "Harmonics and Inter-harmonics of Voltage Converter Supplied Induction Machine Stator Currents". ICREPQ'07, Sevilla 28-30 of March, 2007. Pr., pp. 25-26.
- [2] Rusek, J.: "Category, slot harmonics and the torque of induction machines". COMPEL, Emerald, England, .: vol.22, no 2, 2003, pp. 388-409.
- [3] Rusek J., "Categorization of induction machines in current signature analysis", Electrical Engineering 84 (2002) 265 - 273.

Acknowledgement

This work was supported by AGH University of Science and Technology *Statute Work* number 11.11.120.608.